Supporting information (SI) for:

Synthesis, X-ray structures and magnetic properties of Ni(II) complexes of heteroaromatic hydrazone

Tanja Keškić,[a] Zvonko Jagličić,[b] Andrej Pevec,[c] Božidar Čobeljić,[a] Dušanka Radanović,[d] Maja Gruden,[a] Iztok Turel,[c] Katarina Anđelković,[a] Ilija Brčeski[a,*] and Matija Zlatar[d,*]

[a]*University of Belgrade-Faculty of Chemistry, Studentski trg 12-16, 11000 Belgrade, Serbia*

[b]*Institute of Mathematics, Physics and Mechanics & Faculty of Civil and Geodetic Engineering, University of Ljubljana, Jadranska 19, Ljubljana, Slovenia*

[c]*Faculty of Chemistry and Chemical Technology, University of Ljubljana, Večna pot 113, 1000 Ljubljana, Slovenia*

[d]*University of Belgrade-Institute of Chemistry, Technology and Metallurgy, National Institute of the Republic of Serbia, Njegoševa 12, 11000 Belgrade, Serbia*

*Corresponding authors:

Ilija Brčeski: ibrceski@chem.bg.ac.rs

Matija Zlatar: matijaz@chem.bg.ac.rs; matija.zlatar@ihtm.bg.ac.rs

Table S1. Structural and magnetic parameters of related bis(μ-$_{1,1}$-azido) bridged Ni(II) complexes.

Table S2. Hydrogen-bond parameters for complex **1a**.

Table S3. Hydrogen-bond parameters for complex **1b**.

Figure S1. Crystal packing of **1a** showing a) the dimers of **1a** self-assembled within a layer parallel with the (001) lattice plane (view along *c* axis) and b) the role of solvent water molecule (side view).

Figure S2. Crystal packing of **1b** showing dimeric units connected by heterodromic water cycles. a) View along *b* axis. b) View along *c* axis.

Table S4. Calculated Mulliken Ni(II) spin population values in the ferromagnetic states for 19 Ni(II) binuclear complexes with different DFAs.

Figure S3. Model systems based on crystal structure of **1a**

Figure S4. Model systems based on crystal structure of **1b**

Table S5. Energy Decomposition Analysis at BP86-D4/TZP level of theory of bonding between monomeric structures of **1a** and **1b** with H_2O

Figure S5. Most important density deformation channels from EDA–NOCV analysis of the interaction of monomeric structures of **1a** and **1b** with H_2O.

Table S1. Structural and magnetic parameters of related bis(μ-$_{1,1}$-azido) bridged Ni(II) complexes.

Complex	Ni–$N_{azido(end-on)}$–Ni (°) (mean value)	Ni···Ni (Å)	Ni–$N_{azido(end-on)}$ (Å)	$N_{azido(terminal)}$–Ni–$N_{azido(end-on)}$–Ni (°)	δ(°)[a]	J (cm^{-1})	Ref.
Ligand (**L**) function:							
Tridentate							
$[Ni_2(\mathbf{L}^3)_2(N_3)_4]\cdot H_2O\cdot CH_3OH$[b] (**I**)	102.11(7), 102.01(8) (102.06)	3.281	2.085(2) 2.140(2) 2.134(2) 2.082(2)	−21.4(5), −179.82(9), −179.07(9), −19.6(6)	36.69(16) 0.05(16)	+12.0(2)	[1]
$[Ni_2(\mathbf{L}^4)_2(N_3)_4]$[c] (**II**)	99.7(4)	3.191(4)	2.086(8), 2.088(9)	93.4(3), −89.7(3)	27.2(6)	+34.2	[2]
$[Ni_2(\mathbf{L}^5)_2(N_3)_4]$[d] (**III**)	101.3(1), 100.0(1) (100.65), 97.6(1)	3.296, 3.221	2.085(2), 2.117(2), 2.184(2), 2.176(2), 2.180(2), 2.101(2)	102.9(1), −100.8(1), −82.6(1), 78.9(1), 87.6(1), −89.8(1)	25.78(16) 33.19(16) 40.44(16)	+11.35	[2]
$[Ni_2(\mathbf{L}^6)_2(N_3)_4]\cdot CH_3OH$[e] (**IV**)	103.3, 100.3 (101.79)	3.395, 3.333	2.155(3), 2.142(3), 2.174(3), 2.200(3)	96.3(2), −92.9(2), 92.7(1), −91.4(1)	35.7(2) 24.8(3)	+1.91	[3]
$[Ni_2(\mathbf{L}^7)_2(N_3)_4]\cdot H_2O$[f] (**V**)	98.7(2), 98.5(2) (98.6)	3.190(1)	2.075(4), 2.080(4), 2.132(4), 2.131(4)	21.0(2), 165.9(2), 161.2(2), −9.5(9)	8.3(3) 25.2(3)	+28.32	[4]
$[Ni_2(\mathbf{L}^8)_2(N_3)_4]\cdot 1.5H_2O$[g] (**VI**)	103.9(1)	3.3522(7)	2.138(3), 2.120(3)	−83.8(1), 90.7(1)	18.8(2)	+25.50	[5]
$[Ni_2(\mathbf{L}^9)_2(N_3)_4]$[h] (**VII**)	102.2(2), 101.0(2) (101.6)	3.297(1)	2.109(5), 2.163(6), 2.128(6), 2.107(5)	20.0(2), −177.0(3), −11.0(3), 179.5(3)	18.0(5) 18.1(5)	+36.3	[6]
$[Ni_2(\mathbf{L}^{10})_2(N_3)_4]\cdot H_2O$[i] (**VIII**)	101.6(1)	3.274(1)	2.039(3), 2.184(3)	−179.8(2), 2.0(1)	15.0(3)	+22.8	[7]
$[Ni_2(\mathbf{L}^{11})_2(N_3)_4]$[j] (**IX**)	103.7(1)	3.448(1)	2.217(4), 2.169(4)	−178.4(2), 8.9(9)	12.3(3)	+23.35	[8]
$[Ni_2(\mathbf{L}^{12})_2(N_3)_4]$[k] (**X**)	98.98(5)	3.2362(3)	2.1598(12), 2.0964(12)	89.57(5), −87.57(5)	25.05(8)	+18.61	[9]
$[Ni_2(\mathbf{L}^{13})_2(N_3)_4]$[l] (**XI**)	98.36(9)	3.2394(4)	2.192(2), 2.087(2)	89.2(1), −89.4(1)	33.4(2)	+31.87	[9]
$[Ni_2(\mathbf{L}^{14})_2(N_3)_4]$[m] (**XII**)	100.73	3.2511(6)	2.136(3), 2.085(3)	179.0(1), −7.0(1)	39.0(2)	+16.87	[10]
$[Ni_2(\mathbf{L}^{15})_2(N_3)_4]$[n] (**XIII**)	98.7(2), 101.0(2) (99.85)	3.209(1) 3.236(1)	2.103(4) 2.127(4) 2.052(5) 2.143(5)	89.1(2), −91.0(2), −92.5(2), 90.8(2)	3.0(5), 21.5(3)	+33.0	[11]
$[Ni_2(\mathbf{L}^{16})_2(N_3)_4]$[o] CH_3OH(**XIV**)	100.22(5), 102.29(6) (101.25)	3.264(1)	2.1306(13) 2.0920(12) 2.0988(13) 2.1228(13)	−103.59(5), 107.73(6), −78.08(6), 83.49(6)	20.61(10) 15.09(9)	+24.9	[12]
$[Ni_2(\mathbf{L}^{17})2(\mu\text{-}_{1,1}\text{-}N_3)_2(N_3)_2]$ (**XV**)	102.0(3)	3.305	2.073(6)	–179.7(3), 179.6(4), 2(2), 0.4(4)	15.83	+6.1	[13]
Bis-tridentate							

$[Ni_2(\mathbf{L}^{18})(N_3)_4]^q$ (**XVI**)	98.36(8), 97.66(9) (98.01)	3.155	2.061(2), 2.061(2), 2.108(2), 2.130(2)	3.5(7), 159.1(1), 10.0(7), 160.0(1)	8.9(2) 39.7(2)	+21.8	[14]
$[Ni_2(\mathbf{L}^{19})(N_3)_4]^r$ (**XVII**)	101.7(2), 101.1(2) (101.4)	3.330(1)	2.152(6), 2.150(6), 2.144(6), 2.159(6)	−177.5(3), 1.0(2), −177.2(3), 3.0(2)	32.9(5) 33.4(4)	+20.96	[15]

[a] δ(°) is the out-of-plane deviation of the azide ion measured as the angle between Ni_2N_2 plane and the N–N bond.

[b] $\mathbf{L}^3$ = condensation product of 2-quinolinecarboxaldehyde and trimethylammonium acetohydrazide chloride.

[c] $\mathbf{L}^4$ = *N*,*N*-bis(2-pyridylmethyl)amine.

[d] $\mathbf{L}^5$ = *N*-(2-pyridylmethyl)-*N*′,*N*′-diethylethylenediamine.

[e] $\mathbf{L}^6$ = *N*,*N*-dimethyl-*N*′-(pyrid-2-ylmethyl)-ethylenediamine.

[f] $\mathbf{L}^7$ = 2-[(2-hydroxypropylimino)methyl]phenol.

[g] $\mathbf{L}^8$ = bis(2-(3,5-dimethyl-1*H*-pyrazol-1-yl)ethyl)amine.

[h] $\mathbf{L}^9$ = *N*′-(2-pyridin-2-ylethyl)pyridine-2-carbaldimine.

[i] $\mathbf{L}^{10}$ = 2,2′:6′,2′′-terpyridine.

[j] $\mathbf{L}^{11}$ = methylbis-(3-aminopropyl)amine.

[k] $\mathbf{L}^{12}$ = *N*,*N*-diethyl-*N*′-((3,5-dimethyl-*1H*-pyrazol-1-yl)methyl)ethane-1,2-diamine.

[l] $\mathbf{L}^{13}$ = *N*-((*1H*-pyrazol-1-yl)methyl)-*N*′,*N*′-diethylethane-1,2-diamine.

[m] $\mathbf{L}^{14}$ = 1-Ethyl-2-[*o*-(thiomethyl)phenylazo]imidazole.

[n] $\mathbf{L}^{15}$ = *N*-(2-pyridylmethyl)-*N'*-(2-hydroxyethyl)ethylenediamine.

[o] $\mathbf{L}^{16}$ = 2-methyl-2-[(2-pyridinylmethyl)amino]-1-propanol.

[p] $\mathbf{L}^{17}$ = (*E*)-1-(pyridin-2-yl)-*N*-(quinolin-8-yl)methanimine.

[q] $\mathbf{L}^{18}$ = condensation product of 2-benzoyl pyridine and triethylenetetramine.

[r] $\mathbf{L}^{19}$ = prepared from the reaction of 2-benzoylpyridine with *N*,*N*′-bis-(3-aminopropyl)ethylenediamine.

Table S2. Hydrogen-bond parameters for complex **1a**.

D–H···A	D–H (Å)	H···A (Å)	D···A (Å)	D–H···A (°)	Symm. operation on A
O1W–H1W'···O1W[a]	0.97(15)	2.16(16)	2.863(9)	129(12)	2-x, 1-y, -z
O1W–H2W···N3	0.96(6)	1.95(8)	2.895(6)	170(9)	
C1–H1···N10	0.95	2.50	3.428(7)	165	-1+x, y, z
Intra C5–H5B···S1	0.98	2.75	3.266(6)	114	
C7–H7A···O1	0.99	2.46	3.421(4)	165	2-x,-y,1-z
C8–H8A···N7	0.98	2.55	3.378(6)	143	x,1+y, z
Intra C9–H9A···N7	0.98	2.57	3.459(6)	151	1-x,-y,1-z
C10–H10B···O1W	0.98	2.42	3.334(6)	154	2-x,1-y,-z
C10–H10C···N8	0.98	2.55	3.415(5)	147	2-x,-y,1-z

[a] H1W was refined with 50% occupancy.

Table S3. Hydrogen-bond parameters for complex **1b**.

D–H···A	D–H (Å)	H···A (Å)	D···A (Å)	D–H···A (°)	Symm. operation on A
O1W–H1W···N10	0.94(2)	1.87(2)	2.802(4)	176(3)	x,1/2-y,1/2+z
O1W–H2W···N3	0.92(3)	1.91(3)	2.826(3)	175(3)	
O2W–H3W···O1W	1.01(3)	1.81(3)	2.811(4)	172(3)	2-x,-y,1-z
O2W–H4W···O1W	1.01(4)	1.77(4)	2.744(4)	160(4)	
C1–H1···N7	0.93	2.61	3.450(3)	150	1-x,1/2+y,-1/2-z
Intra C5–H5B···S1	0.96	2.80	3.254(3)	110	
C5–H5B···O2W	0.96	2.57	3.333(5)	136	2-x,1/2+y,1/2-z
C7–H7B···N7	0.97	2.41	3.340(3)	160	x,-1/2-y,1/2+z
Intra C9–H9A···O1	0.96	2.26	2.930(4)	126	
C9–H9C···O2W	0.96	2.39	3.326(5)	164	2-x,-1/2+y,1/2-z

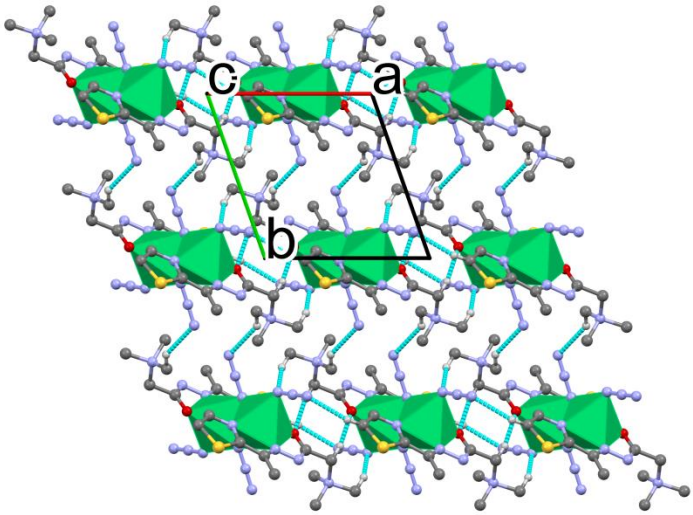

a)

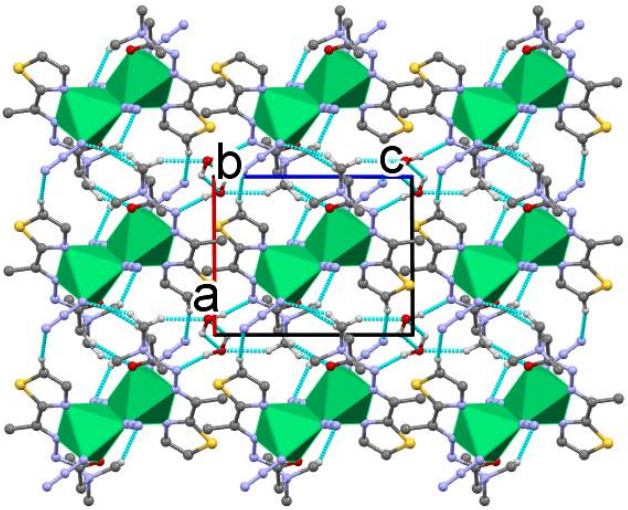

b)

Figure S1. Crystal packing of **1a** showing a) the dimers of **1a** self-assembled within a layer parallel with the (001) lattice plane (view along *c* axis) and b) the role of solvent water molecule (side view). Hydrogen atoms have been omitted for the sake of clarity, except those involved in hydrogen bonding.

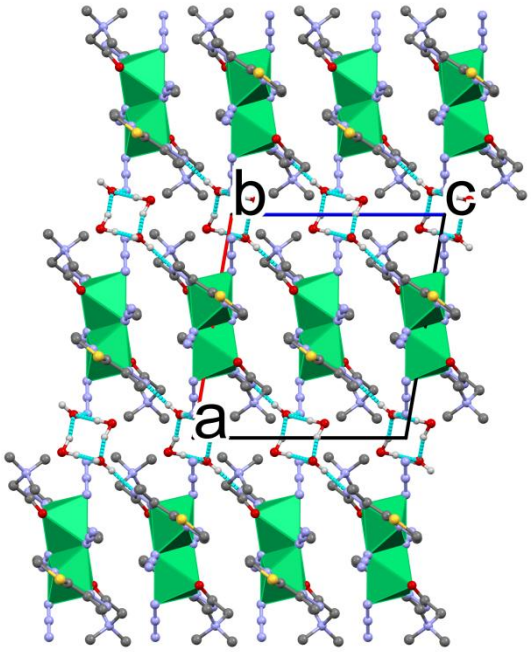

a)

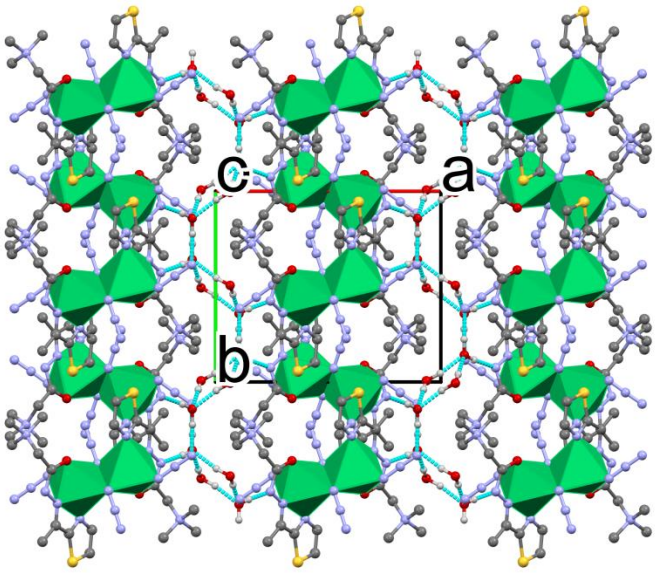

b)

Figure S2. Crystal packing of **1b**showing dimeric units connected by heterodromic water cycles. a) View along *b*axis. b) View along*c* axis. Hydrogen atoms have been omitted for the sake of clarity, except those involved in hydrogen bonding.

Table S4. Calculated Mulliken Ni(II) spin population values in the ferromagnetic states for 19 Ni(II) binuclear complexes with different DFAs. The amount of the exact exchange present in DFA is indicated as % exact X.

Complex	BLYP	TPSSh	B3LYP*	B3LYP	M06	BHandHLYP	M06-2X
% exact X	0	10	15	20	27	50	54
I	1.409	1.567	1.557	1.599	1.590	1.752	1.751
II	1.346	1.502	1.495	1.541	1.532	1.702	1.714
III	1.409	1.551	1.542	1.583	1.527	1.738	1.751
IV	1.378	1.538	1.529	1.577	1.542	1.745	1.753
V	1.462	1.604	1.597	1.635	1.622	1.767	1.771
VI	1.433	1.569	1.558	1.597	1.551	1.742	1.746
VII	1.391	1.541	1.531	1.574	1.558	1.729	1.738
VIII	1.397	1.545	1.536	1.578	1.576	1.732	1.740
IX	1.410	1.555	1.541	1.583	1.555	1.739	1.748
X	1.422	1.559	1.591	1.591	1.522	1.742	1.751
XI	1.411	1.554	1.544	1.586	1.531	1.741	1.751
XII	1.329	1.497	1.485	1.536	1.529	1.723	1.726
XIII	1.402	1.544	1.533	1.574	1.563	1.726	1.735
XIV	1.430	1.571	1.559	1.599	1.586	1.747	1.749
XV	1.373	1.533	1.524	1.569	1.559	1.731	1.748
XVI	1.391	1.539	1.530	1.572	1.545	1.730	1.733
XVII	1.405	1.551	1.541	1.583	1.563	1.738	1.744
XVIII	1.442	1.580	1.571	1.610	1.566	1.754	1.764
XIX	1.445	1.583	1.575	1.614	1.576	1.758	1.768

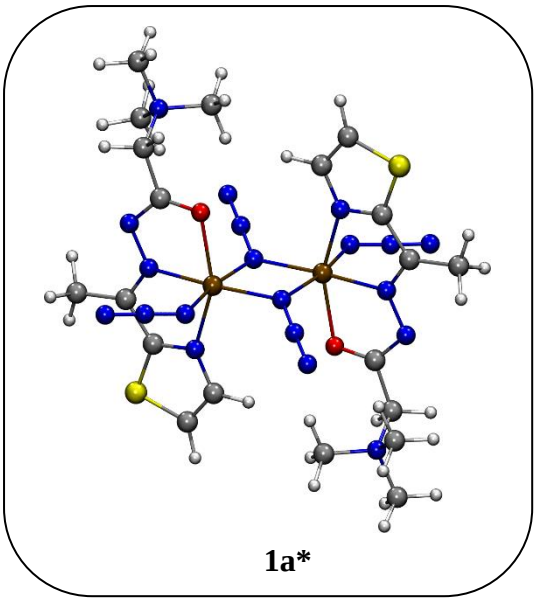

1a*

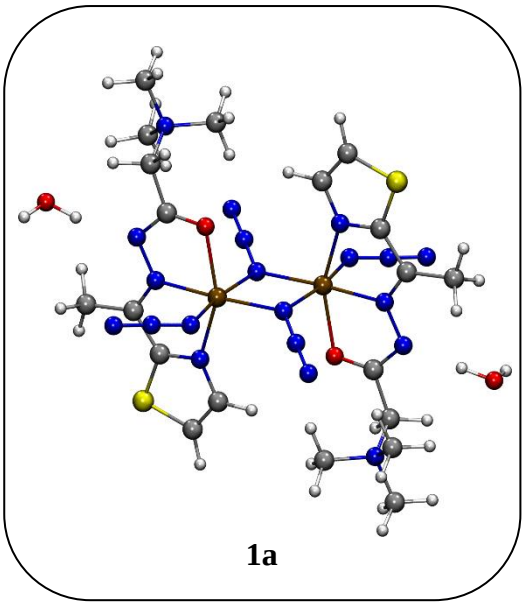

1a

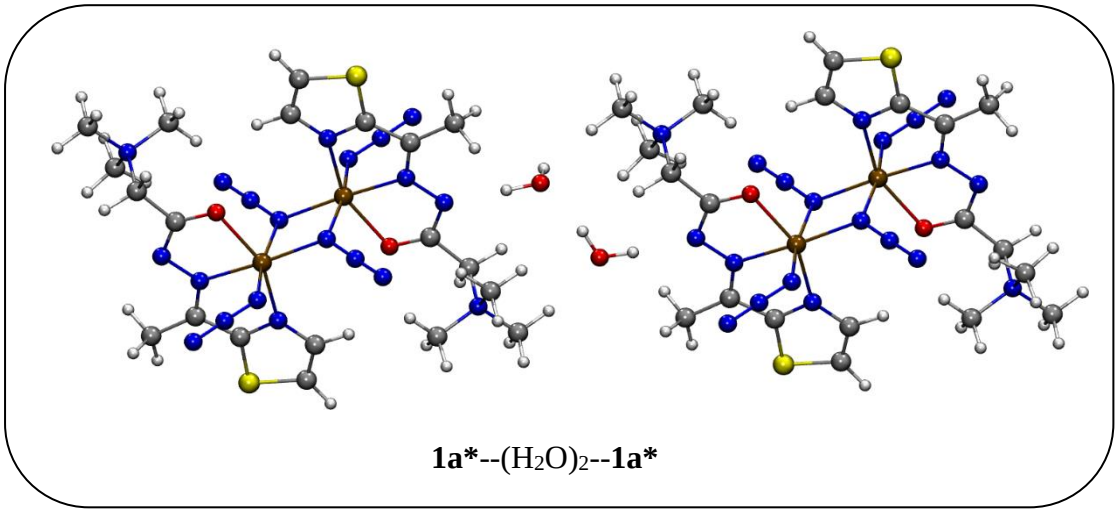

1a*--$(H_2O)_2$--**1a***

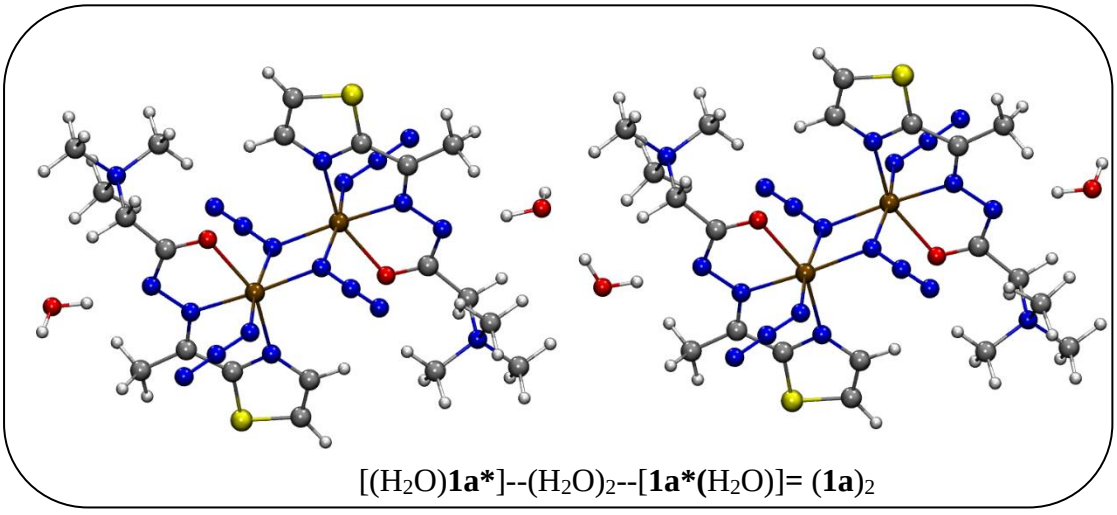

[(H_2O)**1a***]--$(H_2O)_2$--[**1a***(H_2O)]= (**1a**)$_2$

Figure S3 Model systems based on crystal structure of **1a**

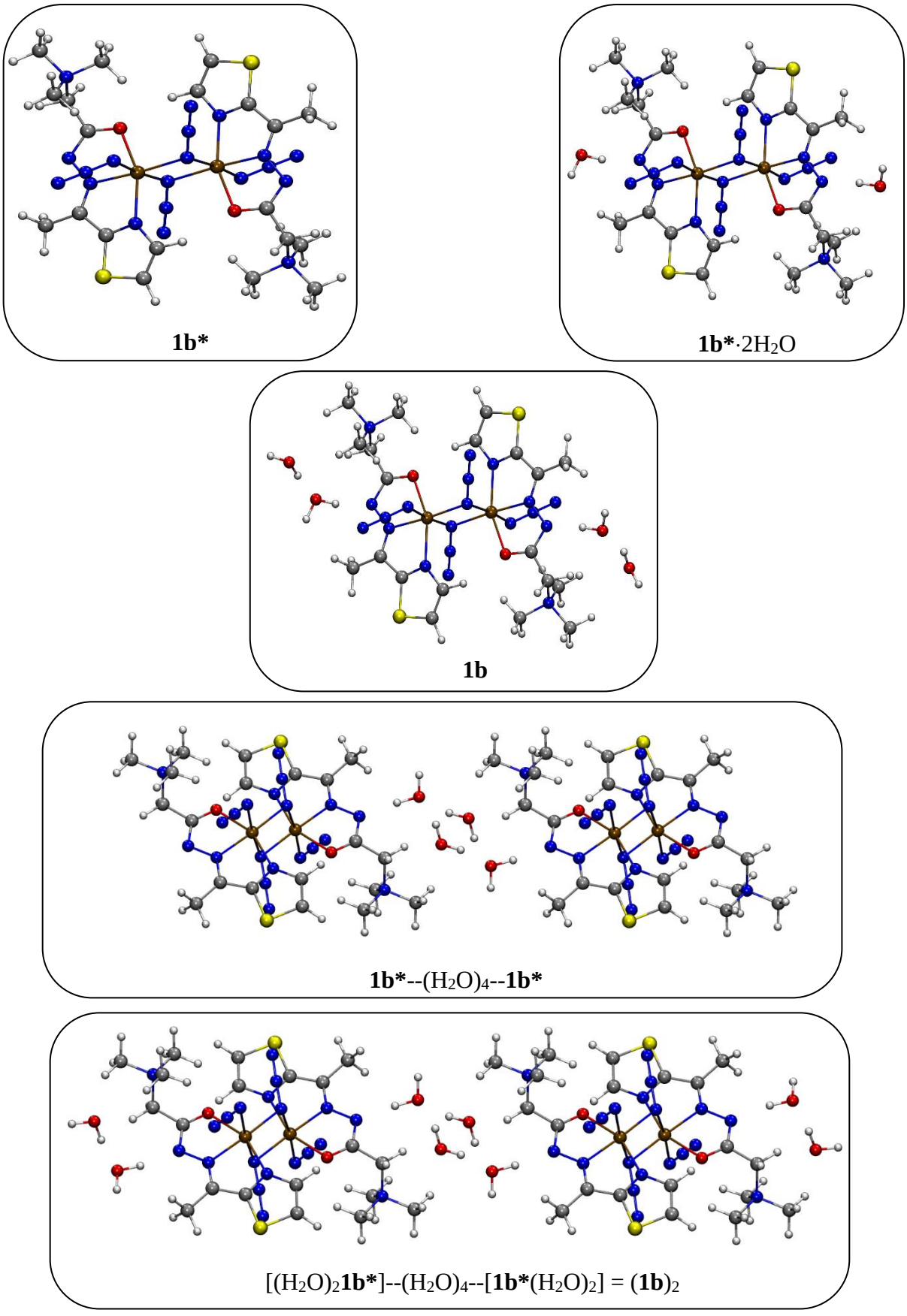

Figure S4. Model systems based on crystal structure of **1b**

Table S5. Energy Decomposition Analysis at BP86-D4/TZP level of theory of bonding between monomeric structures of **1a** and **1b** with H_2O; energy components are given in kcal/mol relative to the chosen fragments; dashed lines indicate fragmentation

	E_{Elst}	E_{Pauli}	E_{Orb}	E_{σ}^{a}	E_{disp}	E_{Int}
1a*--H_2O	-18.09	18.00	-9.73	-6.45	-2.97	-12.8
1b*--H_2O	-17.24	19.15	-10.74	-7.81	-2.62	-11.44
1b*--$(H_2O)_2$	-22.23	21.08	-13.83	-8.81	-4.12	-19.11

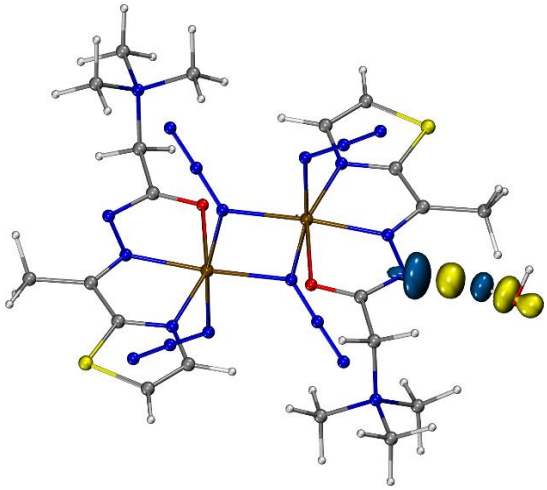

1a*--H_2O E_{σ} = -6.5 kcal/mol

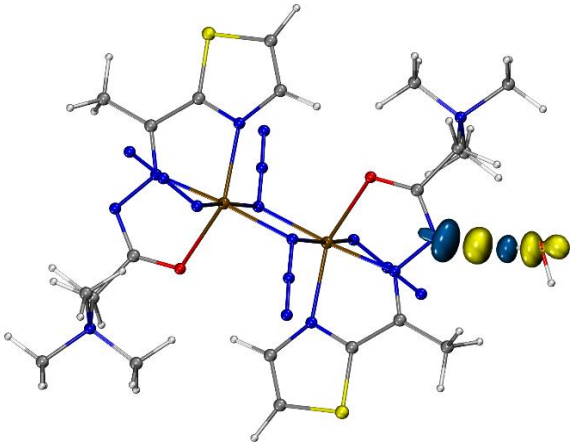

1b*--H_2O E_{σ} = -7.8 kcal/mol

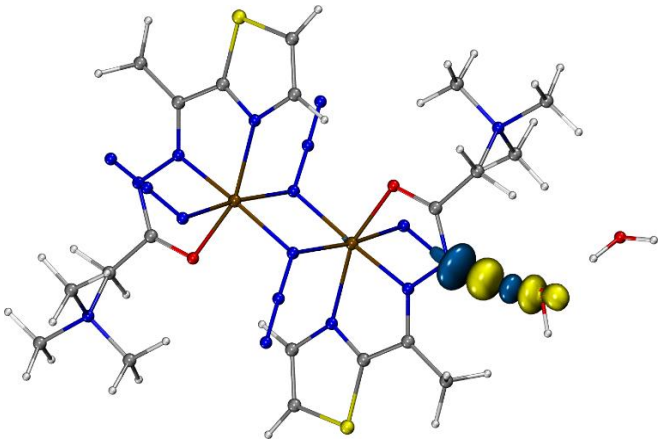

1b*-- $(H_2O)_2$ E_{σ} = -8.8 kcal/mol

Figure S5. Most important density deformation channels from EDA–NOCV analysis of the interaction of monomeric structures of **1a** (up) and **1b** (down) with H_2O. Their relevance is given by their energy contribution E_{σ} to E_{orb}. Charge outflow/inflow is represented by yellow/blue color (isovalue = 0.004 a.u.)

References

[1] M. Č. Romanović, B. R. Čobeljić, A. Pevec, I. Turel, V. Spasojević, A. A. Tsaturyan, I. N. Shcherbakov, K. K. Anđelković, M. Milenković, D. Radanović, M. R. Milenković, Polyhedron 128 (2017) 30–37.

[2] S. Sarkar, A. Mondal, M.S.ElFallah, J. Ribas, D. Chopra, H. Stoeckli-Evans, K.K. Rajak, Polyhedron 25 (2006) 25–30.

[3] H.-D. Bian, W. Gu, Q. Yu, S.-P. Yan, D.-Z. Liao, Z.-H. Jiang, P. Cheng, Polyhedron 24 (2005) 2002– 2008.

[4] S. Liang, Z. Liu, N. Liu, C. Liu, X. Di, J. Zhang, J. Coord. Chem. 63 (2010) 3441–3452.

[5] S.S. Massoud, F.R. Louka, Y.K. Obaid, R. Vicente, J. Ribas, R.C. Fischer, F.A. Mautner, Dalton Trans. 42 (2013) 3968–3978.

[6] R. Cortés, J.I. Ruiz de Larramendi, L. Lezama, T. Rojo, K. Urtiaga, M.I. Arriortua, J. Chem. Soc. Dalton Trans. (1992) 2723–2728.

[7] M.G. Barandika, R. Cortés, L. Lezama, M.K. Urtiaga, M.I. Arriortua, T. Rojo, J. Chem. Soc., Dalton Trans. (1999) 2971−2976.

[8] A. Escuer, R. Vicente, J. Ribas, X. Solans, Inorg. Chem. 34 (1995) 1793–1798.

[9] A. Solanki, M. Monfort, S.B. Kumar, J. Mol. Struct. 1050 (2013) 197–203.

[10] S. Nandi, D. Bannerjee, J.-S. Wu, T.-H. Lu, A.M.Z. Slawin, J.D. Woollins, J. Ribas, C. Sinha, Eur. J. Inorg. Chem. (2009) 3972–3981.

[11] A. R. Jeong, J. W. Shin, J. H. Jeong, K. H. Bok, C. Kim, D. Jeong, J. Cho, S. Hayami, K. S. Min, Chem. Eur. J. 23 (2017) 3023–3033.

[12]A. R. Jeong, J. Choi, Y. Komatsumaru, S. Hayami, K. S. Min, Inorg. Chem. Commun. 86 (2017) 66–69.

[13] P. Ghorai, P. Brandão, S. Benmansour, C.J.G. García, A. Saha, Polyhedron 188 (2020) 114708.

[14] S. Deoghoria, S. Sain, M. Soler, W.T. Wong, G. Christou, S.K. Bera, S.K. Chandra, Polyhedron 22 (2003) 257–262.

[15] S. Sain, S. Bid, A. Usman, H.-K. Fun, G. Aromí, X. Solans, S.K. Chandra, Inorg. Chim. Acta 358 (2005) 3362–3368.